Available online at www.sciencedirect.com

ScienceDirect

Procedia Engineering 10 (2011) 2184–2189

Engineering Procedia

ICM11

The Effect of Mandrel Speed upon the Residual Stress Distribution around Cold Expanded Hole

Kh. Farhangdoost[a] and A. Hosseini[b] *

[a] *Associate Professor, Ferdowsi University of Mashhad / Mechanical Engineering Department, Mashhad, Iran*
[b] *M.Sc Student, Ferdowsi University of Mashhad / Mechanical Engineering Department, Mashhad, Iran*

Abstract

In this paper, cold expansion process on aluminum alloy 2A12TA was simulated using ABAQUS finite element package and the effect of different mandrel speeds upon residual stress distribution around cold expanded hole was considered. The results gained by simulation show major difference between the diagrams of residual stress distribution corresponding different mandrel speeds. The results of FE simulation in slowly loaded process was verified by experimental data. As can be seen, when mandrel speed increases the residual stress around cold expanded hole increases as well and this is caused the fatigue life improvement of fasten holes.

© 2011 Published by Elsevier Ltd. Selection and peer-review under responsibility of ICM11

Keywords: Mandrel speed; Cold expansion; FE; Residual stress.

1. Introduction

With the development of technology, cold expanded holes in aircraft structures play a significant role in design and manufacturing. In fact, residual stresses are induced by cold expansion process in somehow improve fatigue life of fasten holes. So requirement for the fatigue property of key components is more and more strict [10]. Aircraft structures are made up of assembly parts that are riveted or bolted together. Attaching holes are a necessary part of the design. However, stress concentrate around these holes and applied cyclic tensile loads are some fatigue process factors. Over a period of time fatigue process caused fatigue failure of the structure.

* *Corresponding author. Tel.: +98-511-8792783; fax: +98-511-8763304.*
E-mail address: Abbas.Hosseini@stu-mail.um.ac.ir

1877–7058 © 2011 Published by Elsevier Ltd.
doi:10.1016/j.proeng.2011.04.361

According to statistic information from [6], fatigue fracture of fasten holes account for 50–90% of fracture of aging plane, and surface finish of fasten holes have direct effect on usage and reliability of aircraft. Over the last 30 years, the cold expansion process has been widely used to improve the fatigue life of components containing fasten holes without any weight penalty [10]. To achieve cold expansion, an oversized ball or a mandrel can be forced through the hold locally yielding the material to create a plastic region and resulting in internal compressive residual stress. The fatigue life improvement of cold expanded fasten holes is affected of the percentage of compressive residual stress induced through cold expansion [10]. It helps reduce the stress concentration inherent with such holes because of compressive residual stress around the holes surface [3, 8]. Compressive residual stress is mainly affected by several parameters such as diametrical interface, mandrel speed, and temperature and so on. In the pervious studies, diametrical interface [10], temperature [9] and the other parameters have been studied, whereas the effect of mandrel speed has not been thoroughly investigated; however, it has a remarkable effect upon the residual stress distribution around cold expanded hole.

In the aerospace industry, diametrical interferences between 2 and 6% are used for cold expansion [3]. Cold expansion can be achieved in several different ways. There are two main cold expansion techniques: direct cold expansion (without sleeve) and cold expansion using the split-sleeve process [5, 14].

In this paper, cold expanding a hole was carried out using direct cold expansion with 6% diametrical interface since in FE analysis, the direct cold expansion is easier carried out compared to using the split-sleeve process [10].

The main objective of this study is to consider the effect of mandrel speed upon the residual stress distribution around cold expanded hole. To simulate the quasi-static and dynamic processes, ABAQUS/Explicit is one of the most common choices, whereas the lack of precision in this kind of FE software's has been reported by [7]. For this investigation, a novel analytical-numerical method was devised using ABAQUS/Standard in order to investigate the effect of mandrel speed. In this method, ABAQUS/Standard was used instead of ABAQUS/Explicit under the following condition: Material properties were affected by the strain rate in different mandrel speeds. Then, the result for material properties was validated by the experimental data [12, 13]. To show the accuracy of FE model, results gained in slowly loaded process, *v*, were compared with experimental data presented in [10] and an acceptable agreement was achieved.

2. Material Property and Cold Expansion Parameters

2.1. Material properties

The material used for this study was aluminum alloy 2A12T4, with chemical composition, 93% Al, 4.29% Cu, 1.34% Mg, 0.46% Mn, 0.14% Si, 0.31% Fe, 0.02% Ti. Some of the mechanical properties of the material were obtained from tensile test in the rolling direction and stress-strain values are tabulated in Table 1.

For theorical computations [4] and FE simulations, it is often necessary to represent an experimentally determined stress-strain curve by an empirical equation of suitable form. When the material is rigid-plastic, it is frequently convenient to employ the Ludwick Power Law:

$$\sigma = k\varepsilon^n \tag{1}$$

Where k is constant stress and n is a strain-hardening exponent usually lying between zero and 0.5. According to experimental data presented in Table 1 and using the least squares method, the stress-strain equation was derived:

Table 1. Experimental data from tensile test

Strain	Stress(Mpa)
0.01	346.15
0.02	370.19
0.03	394.23
0.04	402.91
0.05	413.59
0.06	417.47
0.07	427.18

$$\log(\sigma) = \log(k) + n\log(\varepsilon) \tag{2}$$

$$\log(\sigma) = Y\ ,\ \log(k) = B\ ,\ \log(\varepsilon) = X\ ,\ n = A \tag{3}$$

$$Y = AX + B \tag{4}$$

$$S = \sum_{i=1}^{7} (Y_i - f(x_i))^2 \tag{5}$$

$$\frac{\partial S}{\partial A} = 0 \tag{6}$$

$$\frac{\partial S}{\partial B} = 0 \tag{7}$$

$$\sigma = (570.5582)\varepsilon^{0.1089} \tag{8}$$

For many materials at room temperature, the properties measured will not vary greatly with small changes in loading speed or deformation rate [11]. If loading speed or deformation rate, v, is suddenly changed by a factor of 10 or more, a small jump in the load may be observed. This indicates some strain-rate sensitivity in the material that can be described by the exponent, m, in the equation:

$$\sigma = k\varepsilon^n \dot{\varepsilon}^m \tag{9}$$

The strain rate is:

$$\dot{\varepsilon} = \frac{d\varepsilon}{dt} = \frac{\frac{dl}{l}}{dt} = \frac{1}{l} \times \frac{dl}{dt} = \frac{v}{l} \tag{10}$$

Where, l denotes the length of the parallel reduced section of the test-piece. If the loading speed, v, increases with the increase of the length of parallel reduced section, l then the strain rate will be constant during the process; therefore, the following equation can be derived:

$$\dot{\varepsilon} = c \tag{11}$$

$$\sigma = (k\,c)\,\varepsilon^n \tag{12}$$

Experiments performed on the effect of strain rate upon material properties show direct relation between coefficient, c, and loading speed, v [12, 13]. In the other words, as loading speed, v, increases, the value of coefficient, c, increases as well. Hence, new stress-strain equations corresponding different loading speeds will be derived [12, 13]. Here, the loading speeds, v, $10v$, $100v$ were considered and modal stress-strain curves corresponding speeds are depicted in Fig 1.

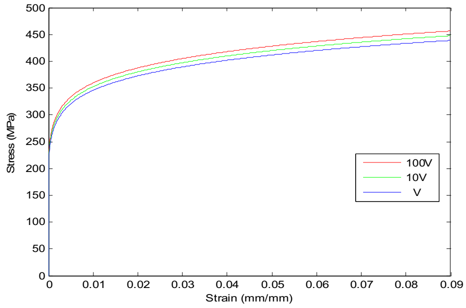

Fig. 1. Stress-strain diagram corresponding to different speeds

In this study, to simulate cold expansion process using ABAQUS/Standard in different mandrel speeds, v, $10v$, $100v$, different stress-strain curves corresponding loading speeds were used. Besides material properties, contact conditions including coefficient of friction should be varied in different mandrel speeds but in this study, the effect of coefficient of friction was ignored because of its insignificant influence on residual stress [6].

2.2. Cold expansion parameter

The alloy was supplied in sheet form 4mm thick and cut into specimen of the form and the final dimensions shown in Fig. 2. It is noted that the axis of loading is parallel to the rolling axis of sheet.

The specimen is cold expanded with pre-drilled hole of 4.8 mm, the largest diameter of mandrel 5.1mm and the interference on holes diameter is 6%.

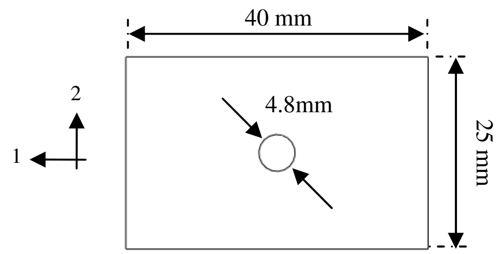

Fig. 2. Specimen in detail accompanied with dimensions

3. FEM Analysis of Residual Stress

Many analytical solutions have been developed to predict the residual stress distribution surrounding cold expanded holes. Two-dimensional model can show acceptable agreement with experimental measurements, but three-dimensional model is used in order to improve the results. The ABAQUS finite element package is used to carry out the analysis [1].

In the ABAQUS element library, ABAQUS linear hexahedron reduced integration elements, C3D8R (three dimensional eight nodded continuum elements), are used to mesh the model. Due to geometry and loading double symmetry with respect to 2–3and 1–3 planes, only one quarter of the plate is needed and the nodes on the planes are constrained from translation perpendicular to the plane and rotation about the in-plane axis but here, the whole model is simulated in order to adapt the results as precise as possible with experimental data.

In a finite element analysis, selection of mesh size and layout is critical. It is desirable to use as many elements as possible in the analysis. However, such an analysis will require excessive computer time. To gain an optimal result without excessive use of computer time, the closer to the hole, the refiner the mesh. After applying the abovementioned conditions, the status of elements can be shown in Fig. 3 (a). In addition, the plate is constrained in the 3-direction at the bottom face for which is in contact with a steel plate. The friction effect between mandrel and hole is ignored in this work because of the insignificant influence of the coefficient of friction on the residual stress [6]. The contact surface of mandrel is set as master face and surface of hole is set as slave face when contact face defined. The simulation of cold expansion is carried out by change the position of mandrel on the 3-direction.

The material of mandrel is steel with Young’s modulus of 210 GPa and Poisson’s ration of 0.3. Linear elastic material relationship is assumed for it. An elastic-plastic material relationship is used to represent the aluminum alloy 2A12T4 with kinematic hardening. Regarding different mandrel speeds, v, $10v$ and $100v$, material relationship varies according to Equation (12).

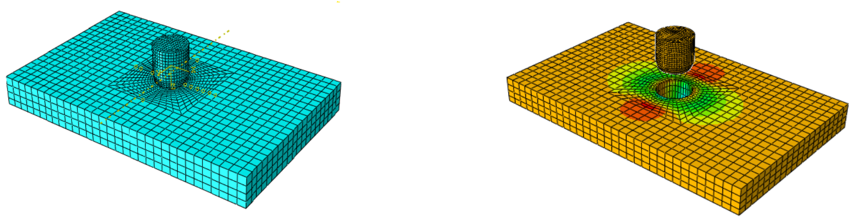

Fig.3. (a) overall orientation of the elements in plate and mandrel; (b) compressive residual stress distribution around cold expanded hole

4. Results of Simulation

After cold expansion simulation, tangential residual stress distribution around cold expanded hole was considered in different mandrel speeds. Unlike geometry and loading double symmetry with respect to 2-3 and 1-3 planes, compressive residual stress is not symmetric in different mandrel speeds. Fig. 3 (b) shows compressive residual stress distribution around cold expanded hole.

The tangential residual stress in different mandrel speeds decreases with distance from the edge hole on 1 and 2-direction. The tangential residual stress distributions in different mandrel speeds are shown in Fig. 4 (a) and (b). As can be seen in diagrams presented in Fig. 4 (a) and (b), the maximum residual stress occurred on the edge hole.

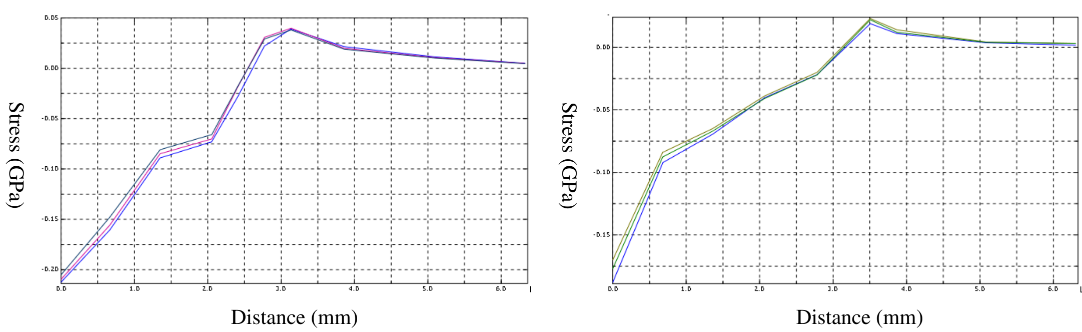

Fig4,(a) residual stress distribution around cold expanded hole on 1-direction, (b) residual stress distribution around cold expanded hole on 2-direction.

When mandrel speed *v* is being considered, the results show that on top face, the zone size of compressive stresses is about 2.7mm on the 1-direction, whereas it is compressive about 3.1mm on the 2-direction. The zone size of compressive stresses is larger on the 2-direction than it is on 1-direction. This result is very agreement with measured results by J. Liu et al.

The magnitude of compressive residual stress on points 1 and 2 for different mandrel speeds is presented in Fig. 5 (b). The configuration of points is shown in Fig. 5 (a).

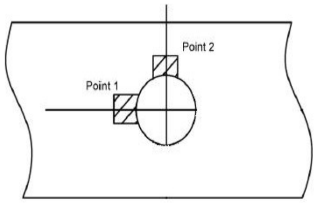

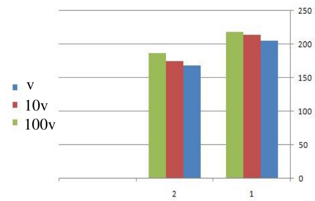

Fig5, (a) overall orientation of the elements in plate and mandrel; (b) The magnitude of compressive residual stress on points 1 and 2 for different mandrel speeds

According to results gained from simulation, as mandrel speed increases the compressive residual stress in 1 and 2-direction increase as well; hence, the size of zone of compressive residual stress gets larger with the increase of mandrel speed. Finally, the improvement of the fatigue life can be observed, obviously.

As mandrel speed is *v* and the effect of strain rate is negligible, the results gained from simulation have partial difference with experimental data. The partial difference is due to ideal condition applied to the simulation. The ideal conditions applied to the simulation are as follows: Uniform loading and boundary conditions. In conclusion, partial difference between simulation and experimental data is natural.

Acknowledgements

The authors gratefully acknowledge Professor Mehran Kadkhodayan and Professor Saeed Hadidi for their appreciable guides.

References

[1] ABAQUS/standard User's Manual, Version 6.1, HKS Inc., 2000.
[2] Arthur P. Boresi, Richard J. Schmidt, Advanced Mechanics of Materials, ISBN 0-471-43881-2
[3] T.N. Chakherlou, J. Vogwell, Eng. Fail. Anal. 10 (2003) 13–24.
[4] J. Chakrabarty, Theory of Plasticity, ISBN 0-7506-6638-2
[5] A.A. Garcia-granada, D.J. Smith, M.J. Pavier, Int. J. Mech. Sci. 42 (2000) 1027–1047.
[6] H.F. Huang, H. Yan, C.H. Tao, J. Mech. Strength 20 (3) (1998), 237–239,215.
[7] M. Kawka, L. Olejnik, A. Rosochowski, H. Sunaga, A. Makinouchi. Journal of Materials Processing Technology 109 (2001) 283-289
[8] V.D. Lacarac, D.J. Smith, M.J. Pavier, et al., Int. J. Fatigue 22 (2000) 189–203.
[9] V. D. Lacarac, D.J. Smith, M.J. Pavier. International Journal of Fatigue 23 (2001) 161-170
[10] J. Liu, X.J. Shao, Y.S. Liu, Z.F. Yue. Material Science 477 (2008) 271-276
[11] Z. Marciniak, J.L. Duncan, S.J. Hu. Mechanics of Sheet Metal Forming, ISBN 0-7506-5300 0
[12] Yuanming Xia, Ying Wang, Yuanxin Zhou, Shaik Jeelani. Material Letter 61 (2007) 213-215
[13] C. Zhang, L. Leonel, D. Guines, E. Rangeau. Journal of Material 209 (2009) 3849-3858
[14] X. Zhang, Z. Wang, Int. J. Fatigue 25 (2003) 1249–1257.